

COMMENT ON CLUSTER ANALYSIS OF RADIO LOOPS IN CMB DATA

R. W. OGBURN IV

Department of Physics, Stanford University, Stanford, CA 94305, USA and
 Kavli Institute for Particle Astrophysics and Cosmology, SLAC National Accelerator Laboratory, 2575 Sand Hill Rd, Menlo Park, CA 94025, USA
Draft version July 23, 2018

ABSTRACT

A recent article (Liu et al. 2014) looks for evidence in the WMAP internal linear combination map (ILC) of unmodeled emission from the galactic radio loop known as Loop I. The statistically strongest result comes from a cluster analysis that tests whether the peak pixels within a 20° annulus at Loop I are preferentially located near the center line of the annulus. From this cluster analysis the authors report a p -value of 0.018% when considering the four highest bins ($75\text{--}87\ \mu\text{K}$). I show that the reported statistical significance has been overestimated. First, the analysis does not correctly select the hottest peaks in the simulated sky realizations; second, it is sensitive to the map pixelization used, and in particular, pixel size used is similar to the relevant clustering distance. I have run 10,000 simulated sky realizations to reproduce the analysis in Liu et al. (2014) and to calculate the effects of incorrect peak selection and of pixelization. Accounting for both of these effects, I find a p -value of $\sim 1\%$, both in the highest-bin test and in the four-bin test. Finally, I note that even under the assumption that Loop I contributes significant power to the ILC map, the observed clustering remains very unlikely. Therefore, a result inconsistent with statistical isotropy is not automatically strong evidence for a detection of Loop I. I suggest additional tests that could clarify the degree to which the cluster analysis supports a detection of Loop I in the CMB map.

1. INTRODUCTION

Several large-scale “Loops” associated with supernovae and other processes within the galaxy have been detected in radio surveys (Berkhuijsen et al. 1971). The most prominent is Loop I, joined by others in many parts of the sky (Wolleben 2007). It has recently been reported (Liu et al. 2014, subsequently abbreviated as *LMS*) that contamination associated with Loop I is also present in the internal linear combination (ILC) map produced from multiple frequencies of the 9-year WMAP data set (Bennett et al. 2013). The presence of such contamination is inferred from the mean temperature and skewness within a small 2° annulus at Loop I, with a 1–3% probability of occurring by chance.

A second type statistic is also used, based on the clustering of high-temperature peaks or “hot spots” around the center line of Loop I. The clustering analysis is similar to one that has previously been used for study of possible foregrounds in the WMAP ILC (Naselsky et al. 2004). It is calculated that the hottest pixels in the ILC map cluster tightly around the center line in a way that is duplicated in only 0.1% of simulations (p -value of 0.1%) for the highest-temperature bin, or p -value of 0.018% when combining four bins.

The structure of this note is as follows. In Section 2 of this note I summarize the cluster analysis used in the *LMS* paper. In Section 3 I show that the published analysis has not correctly selected the “hot spots” for clustering analysis of the 100,000 simulated sky realizations. In Section 4 I recalculate the statistical significance of evidence for Loop I contamination of the ILC, using 10,000 new simulated maps with modified binning. In Section 5 I discuss the dependence of the result on the map pixelization used and calculate the p -values from an additional set of simulations using a finer map. This analysis gives a p -value of $\sim 1\%$. Finally, in Section 6 I discuss the likelihood of the observed values of the clustering statistic with an interpretation as a detection of Loop I.

2. CLUSTER ANALYSIS

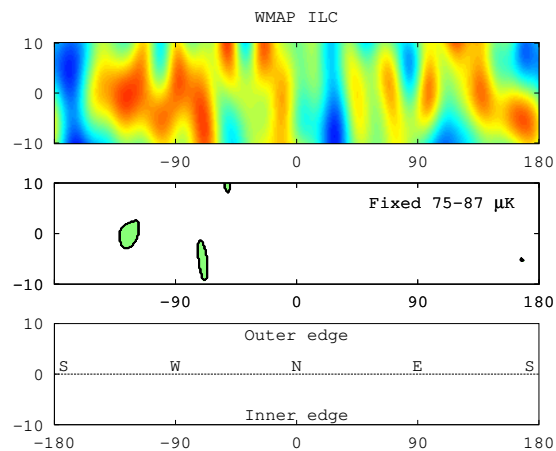


FIG. 1.— WMAP ILC map filtered at $\ell \leq 20$ within the Loop I strip. The data and region selection are the same as in Fig. 2 of *LMS*, but for convenience the annulus is flattened into a strip. The direction toward galactic north is in the center, and the outer edge of the strip is at the top. The color scale in the temperature map (*top panel*) is $[-130, +130\ \mu\text{K}]$. The temperature range $75 \leq T < 87\ \mu\text{K}$ (*middle panel*) contains the four bins used for the clustering analysis in *LMS*. By construction, these bins contain the hottest pixels within the Loop I region.

The cluster analysis in the *LMS* paper uses the WMAP ILC map, filtered to include only multipoles $\ell \leq 20$ and downgraded to NSIDE=128 (Mertsch 2014). An annulus is defined within 10° of the center line of Loop I, according to the parameters in Berkhuijsen et al. (1971). Fig. 1 shows the WMAP ILC map within this region after filtering. I have chosen to flatten the loop into a strip for convenience in comparing the figures. The top panel shows the CMB T map, the middle panel shows the selected hot spots, and the bottom panel indicates the orientation of this flattened strip relative to the sky in galactic coordinates.

The selection of this annulus can be described as follows.

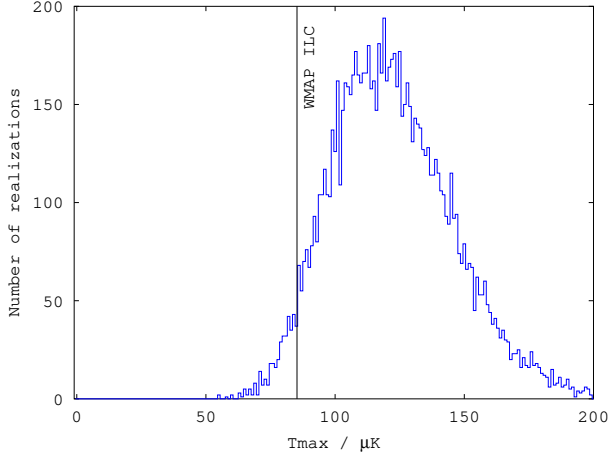


FIG. 2.— Maximum temperature in Loop I annulus in WMAP ILC and simulations

Let P be the set of `Healpix` pixels at NSIDE=128, and \hat{n}_p be the unit vector to the center of any given pixel $p \in P$. Loop I is defined by the unit vector \hat{n}_c of its center at $l = 329^\circ$, $b = +17.5^\circ$ and its radius $r = 58^\circ$. The annulus A is then defined as

$$A = \{p \in P \mid -10^\circ \leq d(\hat{n}_p, \hat{n}_c) - r \leq +10^\circ\} \quad (1)$$

where $d(\hat{n}_1, \hat{n}_2) = \text{Cos}^{-1}(\hat{n}_1 \cdot \hat{n}_2)$ is the great circle distance between two points on the sphere.

For purposes of the cluster analysis the *LMS* authors define bins in CMB temperature with $\Delta T = 3 \mu\text{K}$. The pixels in these bins can be defined as

$$A_i = \{p \in A \mid T_i \leq T(\hat{n}_p) < T_i + \Delta T\} \quad (2)$$

where $T(\hat{n})$ is the temperature in direction \hat{n} in the filtered WMAP ILC map. The highest four bins, $i=1-4$, are intended to select the “hot spots” within the Loop region. The middle panel of Fig. 1 shows the pixels within these four bins, spanning 75–87 μK . The clustering statistic for a single bin is then defined by the average distance of selected pixels from the Loop,

$$G_i = \frac{\sum_{p \in A_i} |d(\hat{n}_p, \hat{n}_c) - r|}{N(p \in A_i)}. \quad (3)$$

The *LMS* paper uses G_i for the clustering statistic defined relative to the filtered WMAP ILC map, and g_i for the same statistic defined relative to a simulated sky realization prepared in the same way as the ILC map, with pixels selected according to Eq. 1. In all cases the bins are defined using fixed bin lower edges $T_i = 75, 78, 81$, and $84 \mu\text{K}$ for $i = 1-4$.

For each bin, a low value of G_i indicates that the hottest pixels in the filtered WMAP ILC map are clustered near the Loop location. This is compared with the equivalent values g_i in the simulated sky realizations. The p -value is calculated as the fraction of simulated realizations for which $g_i < G_i$. The p -values from *LMS* are summarized in Tab. 1. The majority of the statistical power in the cluster analysis comes from the highest bin, $84 \leq T < 87 \mu\text{K}$, containing the hottest parts of the hot spots. This bin has clustering statistic $G_1 = 0.517^\circ$.

3. SELECTION OF HOTTEST PIXELS

I have compared the properties of the WMAP ILC map using 10,000 simulated sky realizations generated with `Synfast` from the `Healpix` package (Górski et al. 2005), then filtered

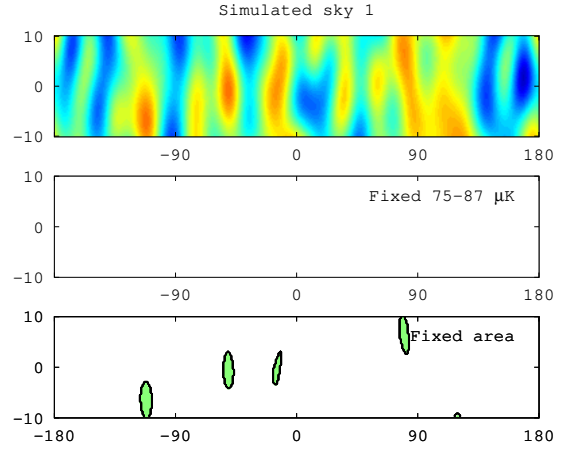


FIG. 3.— One simulated sky realization within the Loop I strip. The color scale in the temperature map (*top panel*) is $[-130, +130 \mu\text{K}]$. This realization has T_{max} lower than in the ILC map, and has no pixels within the range $75 \leq T < 87 \mu\text{K}$ (*middle panel*). About 3.3% of the simulated sky maps fall into this category. The analysis in *LMS* has counted them as less strongly clustered than in the ILC map. The peaks can correctly be selected by taking the hottest pixels up to a fixed area (*bottom panel*).

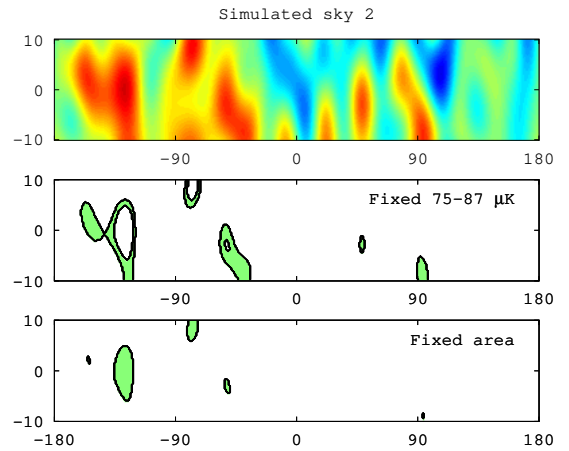


FIG. 4.— A second simulated sky realization within the Loop I strip. The color scale in the temperature map (*top panel*) is $[-130, +130 \mu\text{K}]$. This realization has T_{max} higher than in the ILC map. The temperature range $75 \leq T < 87 \mu\text{K}$ (*middle panel*) does not contain the hottest pixels, but instead selects moderately warm regions that are extended in shape and cover a large solid angle. About 63% of the simulated sky maps fall into this category. The true peaks can be selected by taking the hottest pixels up to a fixed area (*bottom panel*).

to $\ell \leq 20$ and downgraded to NSIDE=128, as in *LMS*. This same set of 10,000 simulations will be analyzed in several different ways to reproduce and test the *LMS* cluster analysis. These maps show a wide variation in the temperature of the hottest pixel, as in Fig. 2. The hottest single pixel in the annulus in the filtered WMAP ILC map has $T = 85.24 \mu\text{K}$. Across simulated realizations, the mean value of the hottest pixel temperature is $\sim 120 \mu\text{K}$. For 96% of the simulated realizations, the hottest pixel temperature is higher than that of the WMAP ILC map. This does not indicate any inconsistency between the real sky and the simulations, but simply shows that the peaks in different realizations are found at different temperatures, typically 60–200 μK .

Although the peak temperatures are different in different realizations, the analysis in *LMS* has used fixed bins in the range $75\text{--}87\ \mu\text{K}$. Because these bins have been chosen with reference to the WMAP ILC map, they will contain the hot spots for this map. However, the hottest pixels do not generally fall into these bins for a simulated sky map. I show two such mock maps in Fig. 3 and Fig. 4. The first of these has a somewhat lower T_{max} than the WMAP ILC map, and as a result has zero pixels within the four bins. Of the 10,000 realizations calculated here, 334 (3.3%) fall into this category, represented by the example in Fig. 3.

A much larger number of simulated maps – most of the realizations – have a higher- T hottest pixel, as shown in the representative example in Fig. 4. These have a large number of pixels within the four used bins, but they do not include the peaks. Instead, these bins now select a range of moderately warm spots that run around the peaks as shown in the middle panel of Fig. 4. These regions are by nature extended rather than localized, and their extended structure gives high values of the clustering statistic g_i . A total of 6273 realizations (63%) fall into this category, defined as those realizations with at least 100 pixels in the $84\text{--}87\ \mu\text{K}$ bin (compared to 33 pixels in the WMAP ILC map).

The use of fixed-temperature bins therefore represents an unfair tailoring of the analysis to the WMAP ILC map, since the bins are guaranteed to identify the peaks in the ILC map but not in the simulations. A simulation whose hottest pixels do (by chance) cluster at the Loop location will typically not have a low value of g_i unless its hottest pixels also (again by chance) have a temperature between 84 and $87\ \mu\text{K}$. The comparison of g_i from the simulations with G_i from the ILC as performed in *LMS* therefore fails to give a correct estimate of the likelihood of the observed clustering. In the next section I propose a modified binning that selects the peak pixels in each realization, and I calculate corrected p -values.

4. MODIFIED PEAK SELECTION

To calculate a correct statistic, one should select the pixels in the simulated maps in a way that matches the treatment of the real data. A simple and valid way to do this is to choose the hottest N pixels, where N is taken from the number of pixels in the same bin in the ILC map. This is equivalent to choosing the same number of pixels in each realization, so that $N(A_i(j^{\text{th}}\ \text{sim})) = N(A_i(\text{ILC}))$. Using this modified definition, the clustering statistic G_i for the WMAP ILC is unchanged, but the statistics g_i for the simulations are now different.

I have compared the results of cluster analysis on my 10,000 simulated sky realizations, both with the unmodified $75\text{--}87\ \mu\text{K}$ bins and with fixed pixel count in each bin. The results are shown in Fig. 5. The top panel shows the distribution of g_1 simulations and the WMAP ILC map, using fixed $84 \leq T < 87\ \mu\text{K}$ as in *LMS*. The values are grouped around 5° , indicating that the selected pixels are not preferentially located near the center line of the strip or near the edges. This reflects the fact that the selected regions are generally not the hottest pixels, but sinuous intermediate contours as in the middle panel of Fig. 3. The spike at the right side of the histogram represents those realizations that have no pixels within the T -bin.

The results of the modified analysis are shown in the bottom panel of Fig. 5. The g_1 values are now distributed evenly across the interval $0 < g_1 < 10^\circ$, with some pileup near $g_1 = 10$. I have recalculated all the statistics from Table 1

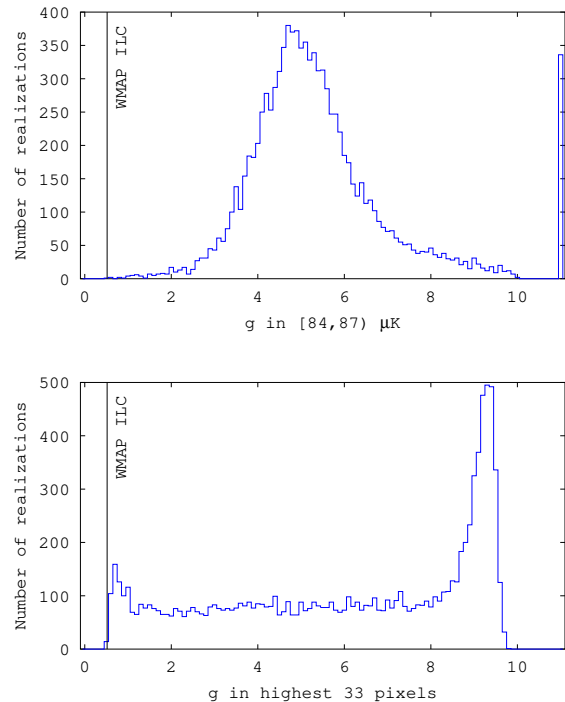


FIG. 5.— Radial clustering statistic as calculated using fixed binning in T , as in *LMS* (top panel), and using a fixed number of pixels (bottom panel). For most realizations, the fixed bins in T contain pixels with moderately warm temperatures and not the true peaks. These have extended patterns that often cross the width of the annulus and give $g_i = 5$. This is the reason for the central distribution in the top panel. A small but significant number of realizations have zero pixels within the bin, and appear here at $g_i = 11$. When the peaks are properly selected in each realization, the distribution of g_i becomes nearly flat. There is a peak at the high end caused by realizations in which the brightest pixels are not local maxima, but sloping edges that intersect the inner or outer edge of the annulus. The smaller peak at the low end corresponds to the minimum value of g_i set by the size of a single hot spot after filtering to $\ell \leq 20$.

of *LMS* after changing the treatment of the simulated maps to select the true hot spots as described above. The results are given in the middle column of Table 1. This calculation shows an overall significance that is weaker than reported in the *LMS* article. The test with all four bins has a recalculated p -value of $\sim 0.1\%$ instead of 10^{-4} .

5. DEPENDENCE ON MAP PIXELIZATION

The clustering statistic G_i is defined in terms of the locations of pixel centers, and the results will therefore depend on the map pixelization used. The analysis in *LMS* uses Healpix maps at NSIDE=128, for which the typical pixel size is $\sim 0.5^\circ$. This is similar to the value of the clustering statistic in the highest temperature bin, $G_1 = 0.517^\circ$. For distances similar to or smaller than the pixel size, the value of G_i is highly sensitive to the locations of the pixel centers relative to the circle defining Loop I. A low value of $G_i \approx 0.5^\circ$ is therefore likely to depend on a coincidental arrangement of Healpix pixels and not only on the properties of the WMAP ILC map.

In order to test this, I have repeated the same analysis at a finer map resolution, NSIDE=512, for which the typical pixel dimension is $\sim 0.1^\circ$. The results are shown in the rightmost column of Table 1, continuing to apply modified binning as in

TABLE 1
PROBABILITY OF $g_i < G_i$ ($i = 1-4$) EVALUATED WITH 10,000
SIMULATIONS

Criterion	Probability	Corrected	
	(<i>LMS</i>)	NSIDE=128	NSIDE=512
$g_i < G_i$ for all 4 bins	0.018%	~ 0.1%	0.5%
$g_i < G_i$ for any 3 in 4 bins	2.0%	5.0%	5.8%
$g_i < G_i$ for any 2 in 4 bins	3.3%	13.9%	13.9%
$g_i < G_i, i = 1$ ($T = 84 \mu\text{K}$)	0.1% ^a	~ 0.1%	1.2%
$g_i < G_i, i = 2$ ($T = 81 \mu\text{K}$)	2.9%	17.0%	17.9%
$g_i < G_i, i = 3$ ($T = 78 \mu\text{K}$)	7.5%	15.4%	14.8%
$g_i < G_i, i = 4$ ($T = 75 \mu\text{K}$)	8.6%	13.9%	14.7%
$\sum_i g_i < \sum_i G_i, i = 1-4$	1.0%	6.7%	7.4%

^aWhen replicating the *LMS* analysis without modification I obtain ~ 0.01% rather than 0.1% as reported in Table 1 of *LMS*.

Section 4. When analyzed at finer map resolution, the clustering values in the ILC map have p -values of 1.2% (highest bin only) or 0.5% (highest four bins) relative to the simulations. This shows that the high significance found by *LMS* is partly attributable to details of the pixelization scheme, and that the significance decreases when working at a map resolution high enough to be insensitive to this effect.

6. LIKELIHOOD UNDER LOOP I INTERPRETATION

The previous sections have shown that the reported significance is reduced after correcting the selection of temperature peaks and using a finer map resolution to avoid pixelization effects. Even after these corrections, the clustering statistic still has a p -value ~ 1%. This remains moderately unlikely under the assumption of statistical isotropy of the CMB as represented by the WMAP ILC map. However, such a result does not automatically constitute a detection of Loop I in the ILC map. It is also necessary to show that a plausible model of contamination from Loop I can account for the low G_i values.

I have tested this using a simple model of Loop I power. Power was added along a thin ring at the coordinates of Loop I, with an amplitude chosen to match the 23.9 μK mean temperature anomaly reported by *LMS*. In an additional 10,000 simulations using modified binning (as in Section 4), at NSIDE=128, I find $g_i < G_i$ in ~ 1% of the realizations. This means that the observed value G_i of the clustering statistic remains unlikely at the ~ 1% level even under a model including power from Loop I in the ILC map. This result could be modified under a different model of Loop I power: for example, one with a variable brightness or anisotropic distribution around the loop. A likelihood ratio test can be used to test

the compatibility of the observed ILC map with a given Loop I model, accounting for any added degrees of freedom in the model.

Such a test should also account for uncertainty in the precise position and shape of Loop I. The position of Loop I is defined by the coordinates listed in Berkhuijsen et al. (1971), which give a center of ($l = 329^\circ \pm 1.5^\circ$, $b = +17.5^\circ \pm 3^\circ$) and a diameter of $116^\circ \pm 4^\circ$. A clustering value of $G_1 = 0.517^\circ$ requires the peaks in the WMAP ILC map to line up with the adopted Loop I center and radius to a precision much finer than the stated uncertainty on these parameters, and even to a level smaller than the number of significant figures with which these parameters have been given. Berkhuijsen et al. (1971) allow the Loop I features to deviate somewhat from ideal circularity and to have finite thickness, stating an RMS deviation of 0.9° , which is less than the value of G_1 in the *LMS* cluster analysis. These effects could be taken into account in a likelihood ratio test by including the center position and radius of Loop I as parameters of the model.

Although a fuller analysis should be performed, a test against a simple model suggests that the observed clustering statistics may be unlikely even under the assumption that Loop I contributes to the ILC map. The uncertainty in the center, radius, and shape of Loop I also indicate that the observed clustering must be attributed at least partly to chance under any such hypothesis.

7. CONCLUSIONS

The significance of clustering evidence for Loop I contamination in the WMAP ILC is overestimated in the *LMS* article because the hottest pixels have not been correctly identified in the simulated sky realizations, and because the coarse map resolution makes the analysis sensitive to details of the pixelization scheme that are not physically meaningful. Accounting for these gives a corrected p -value of ~ 1% rather than the ~ 10^{-4} reported in *LMS*. In addition, it should be demonstrated that the observed clustering values are adequately explained by the interpretation that power from Loop I is present in the WMAP ILC map. In fact, I find that the clustering in the highest bin remains unlikely, and must apparently be attributed to chance even under this interpretation. The consistency of the ILC map with a hypothesis of Loop I power could be tested more quantitatively by performing a likelihood ratio test. The additional analysis presented here does not rule out the existence at some level of contamination from Loop I in the WMAP ILC map, but it does greatly reduce the statistical significance attached to claimed evidence for such contamination.

I acknowledge support from a KIPAC Kavli Fellowship and the Department of Energy. I am grateful to Chao-Lin Kuo and Sergi R. Hildebrandt for helpful discussion and comments.

REFERENCES

- Bennett, C. L., Larson, D., Weiland, J. L., et al. 2013, The Astrophysical Journal Supplement Series, 208, 20
 Berkhuijsen, E. M., Haslam, C. G. T., & Salter, C. J. 1971, Astr. & Astroph., 14, 252
 Górski, K. M., Hivon, E., Banday, A. J., et al. 2005, Astrophys. J., 622, 759
 Liu, H., Mertsch, P., & Sarkar, S. 2014, Astrophys. J. Lett., 789, L29
 Mertsch, P. 2014, personal communication
 Naselsky, P. D., Doroshkevich, A. G., & Verkhodanov, O. V. 2004, Monthly Notices of the Royal Astronomical Society, 349, 695
 Wolleben, M. 2007, The Astrophysical Journal, 664, 349